Low expression of Isocitrate Dehydrogenase 1 (IDH1) R132H is associated with advanced pathological features in laryngeal squamous cell carcinoma

Nasrin Shayanfar
Iran University of Medical Sciences
Ali Zare-Mirzaie
Iran University of Medical Sciences
Mahsa Mohammadpour
Tehran University of Medical Sciences
Ensieh Jafari
Noor Danesh University
Amirhosein Mehrtash
Pasteur Institute of Iran
Nikoo Emtiazi (Nikooemtiazi9@gmail.com)
Iran University of Medical Sciences
Fatemeh Tajik
Iran University of Medical Sciences

Research Article

Keywords: Isocitrate dehydrogenase 1 (IDH1), laryngeal squamous cell carcinoma (LSCC), Immunohistochemistry (IHC), Tissue microarray (TMA), polymerase chain reaction (PCR)

Posted Date: July 28th, 2022

DOI: https://doi.org/10.21203/rs.3.rs-1885687/v1

Abstract

Introduction:

Recent developments in genomic sequencing have led to the identification of somatic mutations in isocitrate dehydrogenase 1 (IDH1) in various malignancies. IDH1 R132H is the most common mutation of IDH1, which affects codon 132 and results in the conversion of amino acid residue arginine (R) to histidine (H). The expression and clinical significance of IDH1 R132H in laryngeal squamous cell carcinoma (LSCC) have not been explored.

Methods

The expression pattern and clinical significance of IDH1 R132H were investigated in tissue microarrays (TMAs) of 50 LSCC tumors as well as adjacent normal tissues using immunohistochemistry (IHC). Then the exon of the 12 tumor samples with negative/weak positive staining were sequenced by applying polymerase chain reaction (PCR).

Results

The results demonstrated that the cytoplasmic expression of IDH1 R132H was downregulated in tumor cells compared to adjacent normal tissues. A statistically significant association was found between a low level of cytoplasmic expression of IDH1 R132H protein and advanced histological grade ($p = 0.000$), perineural invasion ($p = 0.019$), and lymph node involvement ($p = 0.000$). The exon4 sequencing results showed that only one sample was positive for IDH1 R132H mutation. IDH1 R132H expression was observed in 39 (78.0%) LSCC samples.

Conclusion

These findings indicate that low cytoplasmic expression of IDH1 R132H has a clinical significance and is associated with more aggressive tumor behavior and progression of LSCC, which can help improve potential treatment in LSCC patients. Further investigations are required to understand the biological function of marker in LSCC.

1. Introduction

Laryngeal cancer is the most common type of head and neck cancer, accounting for approximately 185,000 new cases and 100,000 deaths worldwide in 2020, indicating a high mortality rate (1). Further, it has been estimated that the new diagnosed cases and mortality rates in the USA will be approximately 12,500 and 4,000, respectively, during 2022 (2). The most prevalent subtype of laryngeal cancer (about 95 percent) is laryngeal squamous cell carcinoma (LSCC) (3). Although the survival rate of the LSCC alters from 80 percent in the early stage to less than 50 percent in the advanced stage, the overall 5-year survival rate is about 60% (4). Despite recent advances in the treatment of LSCC, which include surgery, radiotherapy, chemotherapy, and immunotherapy, it's still diagnosed at an advanced stage, making treatment challenging and the prognosis unsatisfactory (5, 6). As a result, the identification of tumor markers provides a valuable and promising tool with greater efficacy that assists in the diagnosis, treatment, and improvement of prognosis.

Isocitrate dehydrogenase (IDH) is an enzyme of the Krebs cycle (TCA cycle), which catalyzes the oxidative decarboxylation of isocitrate and produces α ketoglutarate (α-KG), CO2, as well as NAD(P)H that protects the cells from reactive oxygen species (ROS) (7, 8). There are three different human IDH isoforms, comprising IDH1, IDH2, and IDH3. The location of IDH1 is cytoplasm and peroxisomes, while IDH2 and IDH3 are localized in mitochondria (9). IDH1 and IDH2 are homodimeric and NADP + dependent, reversible catalyzed reactions with no known allosteric modifiers, whereas

IDH3 is heterotetrameric (2α, 1β, 1γ) and NAD^+ dependent, catalyzed irreversibly and regulated by different allosteric effectors (10).

IDH1, the most commonly identified mutated gene, plays an important role in varied cellular functions, including lipid metabolism, glucose sensing, differentiation, DNA repair, and redox states (11, 12). Mutation in IDH1 led to converting α-KG to D isomer of 2-hydroxyglutarate (D2HG). Accumulation of D2HG, an oncometabolite, leads to hypoxia-inducible factor 1α (HIF-1α) degradation and epigenetic alterations such as DNA demethylases, histone modification, and chromatin remodeling. These changes could affect cancer formation and progression (12–14). The fourth exon of the IDH1 gene encodes three arginine residues, namely R100, R109, and R132, that are significant for the proteins' activity (15). IDH1 mutations are heterogenous missense mutations restricted to a single arginine residue, R132, in the active region of the enzyme (16). It has been discovered that there are five distinct R132 mutations that result in different amino acid exchanges, including histidine (R132H), cysteine (R132C), glycine (R132G), leucine (R132L), and serine (R132S), with R132H being the most prominent mutation (17, 18).

A growing body of evidence has indicated that IDH1 mutations are involved in various malignancies (19, 20). For the first time, IDH1 mutation (IDH1 R132C) was recognized in breast and colorectal cancers in 2006 (21). Following that, Parsons et al. found the IDH1 R132H mutation in glioma (22). It was found that mutations in IDH1 occurred in grade 2 and 3 glioma patients and are more frequently in secondary glioma than primary (18, 23). Besides, IDH1 mutations were observed in patients with acute myeloid leukemia (AML) (24), nonepithelial melanoma (25), chondrosarcoma (26), prostate cancer (27), intrahepatic cholangiocarcinoma (28), and etc. It has been found that the rate of IDH1/2 mutations is low (11.8%) in laryngotracheal chondrosarcoma, suggesting a different mode of tumorigenesis needing further investigation (29).

Although the role of IDH1 mutation was examined in various cancers, its role in LSCC is undetermined. Therefore, the current study was designed for the first time to investigate the expression patterns of IDH1 R132H protein expression in a series of LSCC tumor samples, using the immunohistochemistry (IHC) method on tissue microarray (TMA) slides and its association with different clinicopathological parameters, including histological grade, TNM stage, lymphovascular invasion, perineural invasion, and lymph node involvement. We then evaluated the IDH1 R132H mutation in negative and weak positive staining by applying the PCR method. Our findings may help determine the potential utility of this marker in the targeted therapy and diagnosis of LSCC.

2. Methods

2.1. Investigation of IDH1 based on data mining

cBio Cancer Genomics Portal (cBioPortal) (https://www.cbioportal.org/) is an online visual exploration tool for multidimensional cancer genomics data such as The Cancer Genome Atlas (TCGA) (30). Therefore, the IDH1 gene was searched in the cBioPortal database in order to further evaluate the most mutations of this gene and alterations in protein for head and neck cancer tissue samples. Moreover, to investigate the expression of IDH1 in mRNA levels in patients with head and neck cancer, the UCSC Xena Browser database (https://xenabrowser.net/) was applied and constructed boxplot mRNA expression analysis on normal, primary tumor, and metastatic tissues. UCSC Xena for tumor and normal samples obtained from public and private, multi-omic, and clinical/phenotype data such as TCGA and the Genotype-Tissue Expression (GTEx) (31). Finally, investigation of this biomarker as part of the literature review was done in neoplasm diseases class of DisGeNET plug-in (32) as well as protein-protein interaction (PPI) network was found using stringApp)confidence score ≥ 0.4((33) in Cytoscape software (34).

2.2. Patient's characteristics and tumor samples

A total of 50 formalin-fixed paraffin-embedded (FFPE) sample tissues from LSCC samples were collected from the pathology laboratory of Rasoule-e-Akram hospital, Tehran, Iran, from 2018 to 2019. Patients diagnosed with primary LSCC who had undergone laryngectomy surgery but had not received chemotherapy or radiotherapy were considered eligible for participation in this study. In addition, the hematoxylin and eosin (H & E) stained slides and medical archival documents of enrolled patients were retrieved to obtain clinicopathological and demographic data, including gender, age, tumor size, histological grade, TNM stage, lymphovascular invasion, perineural invasion, and lymph node involvement. Ethical approval was attained by the Ethics Committee of the Iran University of Medical Sciences (IR.IUMS.FMD.REC.1399.276) to use the patient's tissues, and assurance was given to keep the patient's information confidential.

2.3. Tissue microarray (TMA) construction

The H&E slides were examined by an expert pathologist (N.Sh) to identify and mark the three most representative areas of the tumor's various regions. Then the selected areas in each block were punched with a diameter of 0.6 mm using TMA equipment (Minicore; Alphelys, France) and precisely transferred into new recipient paraffin TMA blocks. Due to tumor heterogeneity as a major concern throughout the TMA procedure, three copies were constructed from each tumor sample's TMA block. TMA slides were obtained by cutting sections of TMA blocks to a thickness of about 4 μm, which were transferred to an adhesive-coated slide system. Lastly, the mean expression of three cores was calculated for each tissue sample to enhance the accuracy and validity of the data analysis.

2.4. Immunohistochemistry (IHC) staining

After TMA blocks were sectioned, all prepared slides were dewaxed at 60°C for 1 hour, deparaffinized, and rehydrated with xylene and graded ethyl alcohol. In order to suppression endogenous peroxides, 0.3% hydrogen peroxide (H2O2) for 20 min was added into the slides at temperature room. After washing tissue sections in Tris-buffered saline (TBS), antigens were retrieved from tissue slides by autoclaving them for 10 minutes in citrate buffer (pH 6.0). Then, the slides were incubated with primary antibody, GenAb™ Monoclonal Anti-IDH1 R132H [Clone IHC132-1] dilution of 1/100, overnight at 4°C. The next day, TMA sections following three times washing with TBS, were incubated with mouse anti-rabbit secondary antibody for 30 min at room temperature. Then visualized by diaminobenzidine (DAB peroxidase substrate) and counterstained with hematoxylin. Eventually, the slides dehydrated in graded ethylic alcohol, cleared in xylene, and mounted for evaluation. For a negative control, instead of using primary antibody, an incubation with only TBS was carried out.

2.5. Evaluation of immunostaining

The immunostaining of IDH1 R132H on tissue microarray LSCC slides was evaluated by two independent pathologists (N.Sh., and N.E.) through a semiquantitative scoring system, who were blinded to the clinicopathological and prognostic information. A consensus was attained for all tissue samples. Three scoring systems were used to evaluate the level of IDH1 R132H expression: the intensity of staining, the percentage of positive tumor cells, and the H-score. The immunostaining intensity of IDH1 R132H was visually scored as 0, negative or no staining; 1, weak staining; 2, moderate staining; and 3, severe staining. The percentage of positive tumor cells was scored ranging from 0-100% and categorized into four groups as follows: < 25, 25–50%, 51–75%, and > 75%. The total score was determined using the Histochemical score (H-score), which was calculated by multiplying the intensity of the staining and the percentage of positive cells, resulting in a score between 0 and 300 for each core. In the current study, the median H-score was considered to categorize samples as high or low IDH1 R132H expression.

2.6. DNA extraction

Genomic DNA (gDNA) extraction from FFPE was carried out by applying the E.Z.N.A DNA extraction Kit (Omega Bio-Tek, Inc), according to the manufacturer's instructions. Analyzing mutation hotspots within IDH1 exon 4. Proper positive and

negative controls were included in each run. The programs were analyzed by trained personnel. In order to validate the results, gDNA underwent direct sequencing namely sanger sequencing.

2.7. Polymerase Chain Reaction (PCR)

Two primers were used in this protocol. The sense primer sequence was 5 -CGGCTTGTGAGTGGATGC-3 (position 691–710), and the antisense primer was 5 -TGCTTAATGGGTGTAGATAC-3 (position 829–809). The forward and reverse primers amplified a product of approximately 300 bp.

The amplification conditions were: 95^0C for 8 min; 35 cycles at 94^0C for 30 s, 60^0C for 35 s, 72^0C for 45 min, and 72^0C for 5 min. The PCR reaction mixture for the set of primers contained: 12 µl Master AMPLIQON Taq 2x Master Mix Red 1.5 mM Mgcl2, 1 µl of each primer, 6 µl H_2O_2, and 80 ng gDNA in a total volume of 2 µl. The PCR products were purified through ExoI and Fast-AP according to the manufacturer's instructions. The sequencing reaction was performed using BigDye™ Terminator v3.1 Cycle Sequencing Kit (based on manufacturer's instructions) and 2 µl primers. Each amplification contained positive (IDH1 gDNA) and negative (distilled water) controls to exclude cross-over contamination.

2.8. Statistical analysis

All the obtained IHC data were analyzed using SPSS Statistics 25.0 software (IBM, NY, USA). categorical data were reported as N (percent), whereas quantitative data were reported as mean (SD) and median (Q1–Q3). Pearson's 2 and Spearman's correlation tests were employed to determine the significance of the association and correlation between IDH1 R132H protein expression and clinicopathological variables. Moreover, to make pairwise comparisons between the groups, Kruskal–Wallis and Mann–Whitney *U* tests were performed. A *P* value of < 0.05 was regarded as statistically significant. The sequencing data of the PCR was analyzed through Sequencing Analysis software.

3. Results

3.1. Bioinformatics approaches

The IDH1 mutations from 1438 samples in 5 head and neck cancer studies (cBioPortal) indicated 10 missense mutations which led to 5 changes in IDH1 protein (Fig. 1). Also, the results of the TCGA database for 564 tissue samples via UCSC Xena exhibited the mRNA expression level of IDH1 to a small extent was higher in tumor tissues with metastatic feature than primary tissues and normal tissues from patients with head and neck cancer, although was not significant (One-way Anova, $p = 0.08801$ ($f = 2.441$), Fig. 2).

The PPI information from the STRING database indicated IDH1 has a high confidence score with ACO1, ACO2, GOT2, IDH3B, and OGDH, which dysregulation of them have important roles in cancer progression and tumorigenesis (35, 36) (Fig. 3). Also, according to our findings in the literature review and DisGeNET data, the IDH1 gene was investigated in various cancers (37, 38), but in laryngeal cancer has been less research on the expression pattern for protein levels (Fig. 4).

3.2. Patients' characteristics

In this cross-sectional study, the sample population comprised a total of 50 LSCC patients with a mean age of 61 years (SD = 8.33; range 44–78 years). Of them, 49 cases are men (98.0%), and 1 is a woman (2.0%). Out of 50 patients, 29 (58.0%) were ≥ 61 years old and 21 (42.0%) were < 60 years old. The tumor size ranged from 1.5 to 7.5 cm, with a mean tumor size of 3.9 cm. The tumors size was classified into two groups based on the mean size. Overall, 23 (46.0%) cases showed tumor size of less than 3.9 cm, and 27 (54.0%) cases had tumor sizes of more than 3.9 cm.

The histological grade is classified into three groups as follows: well, moderately, and poorly differentiated. There were 31 (62.0%) well-differentiated, 17 (34.0%) moderately differentiated, and 2 (4.0%) poorly differentiated squamous cells. At

the time of diagnosis, primary tumor (PT) stages were 1 (2.0%) pT1, 10 (20.0%) pT2, 22 (44.0%) pT3, and 17 (34.0%) pT4. Lymphovascular invasion and perineural invasion were identified in 2 (4.0%) and 11 (22.0%) patients, respectively. Fifteen (30.0%) cases had lymph node involvement compared to 35 (70.0%) non-involved cases.

The clinicopathological characteristics of our samples are shown in Table 1.

Table 1
Patients and tumor clinicopathological characteristic of laryngeal squamous cell carcinoma (LSCC)

Patients and tumor characteristics	laryngeal SCC, N (%)
Number of samples	50
Mean age, years (range)	61 (44–78)
≤ Mean age	29 (58.0)
> Mean age	21 (42.0)
Sex	49 (98.0)
Male	1 (2.0)
Female	
Mean tumor size (cm) (rang)	3.9 (1.5–7.5)
≤ Mean tumor size	23 (46.0)
> Mean tumor size	27 (54.0)
Histological grade	31 (62.0)
Well differentiated	17 (34.0)
Moderate differentiated	2 (4.0)
Poor differentiated	
Primary tumor (PT) stage	1 (2.0)
pT1	10 (20.0)
pT2	22 (44.0)
pT3	17 (34.0)
pT4	
Lymphovascular invasion	2 (4.0)
Present	48 (96.0)
Absent	
Perineural invasion	11 (22.0)
Present	39 (78.0)
Absent	
Lymph node involvement	15 (30.0)
Yes	35 (70.0)
No	

3.3. Evaluation of IDH1 R132H expression in laryngeal squamous cell carcinoma and adjacent normal tissue samples using IHC

The IDH1 R132H expression level was assessed by utilizing the IHC technique on the TMA section with three varied scoring methods as follows: intensity of staining, percentage of positive tumor cells, and H-score. The IDH1 R132H expression pattern was observed only in the cytoplasm of both LSCC tissue samples and adjacent normal tissues. Based on the median IDH1 R132H H-score value (120) as the cutoff, patients were categorized into either low (≤ median of H-scores) or high (> median of H-scores) expression. A low expression of IDH1 R132H was observed in 29 (58.0%) LSCC samples, whereas higher IDH1 R132H expression was found in 21 (42.0%) samples. Furthermore, LSCC tissue samples showed IDH1 R132H expression with variable staining intensities, including 5 (10.0%) negative, 7 (14.0%) weak, 17 (34.0%) moderate, and 21 (42.0%) strong (Table 2). The mean expression of IDH1 R132H in adjacent normal tissues was higher than in tumor tissues samples (Fig. 5).

Table 2
Cytoplasmic expression of IDH1 R132H (Intensity of staining, percentage of positive tumor cells, and H-score) in laryngeal squamous cell carcinoma (LSCC) samples

Scoring system	Cytoplasmic expression of IDH1, N (%)
Intensity of staining	5 (10.0)
Negative (0)	7 (14.0)
Weak (+ 1)	17 (34.0)
moderate (+ 2)	21 (42.0)
Strong (+ 3)	
Percentage of positive tumor cells	11 (22.0)
< 25%	10 (20.0)
25–50%	12 (24.0)
51–75%	17 (34.0)
> 75%	
H-score cut off	120
Low	29 (58.0)
High	21 (42.0)
Total	50

3.4. Cytoplasmic expression of IDH1 R132H and its association with clinicopathological features of Laryngeal Squamous Cell Carcinoma

To examine the association between IDH1 R132H expression and clinicopathological features, Pearson's $\chi 2$ test was applied. A statistically significant association was observed between the cytoplasmic expression of IDH1 R132H and histological grade of the tumor in terms of intensity ($p = 0.000$) as well as perineural invasion in terms of H-score ($p = 0.019$). Moreover, our analysis showed a significant association between IDH1 R132H expression and lymph node involvement in both terms of intensity and H-score (All $p = 0.000$) in LSCC patients. As exhibited in Table 3, there was no significant association between IDH1 R132H expression and other important clinicopathological characteristics.

Spearman's correlation analysis was also executed to show the correlation between expression of IDH1 R132H and clinicopathological parameters. The results of Spearman's correlation analysis exhibited a significant inverse correlation between IDH1 R132H expression and histological grade ($p = 0.002$), lymph node involvement ($p = 0.000$), as well as perineural invasion ($p = 0.019$). We observed that higher expression of IDH1 R132H correlated with decreased histological grade, lymph node involvement, and perineural invasion. In addition, Kruskal–Wallis and Mann–Whitney *U* tests also showed significant differences between the median level of IDH1 R132H expression and perineural invasion ($p = 0.035$) and histological grade ($p = 0.014$) (Fig. 6).

Table 3
The association between cytoplasmic IDH1 R132H protein expression and clinicopathological characteristic of laryngeal squamous cell carcinoma samples (*P* value; Pearson's $\chi 2$ test)

Characteristics of tumor	Total samples, N%	Intensity of staining *N* (%)				P value	H score (cut off = 120) N (%)		P value
		0 (Negative)	1 + (Weak)	2 + (Moderate)	3 + (Strong)		Low (< 120)	High (> 120)	
Mean age, years (Range)	61 (44–78)	2 (40.0)	6 (85.7)	11 (64.7)	10 (47.6)	0.249	19 (65.5)	10 (47.6)	0.206
≤ Mean age	29 (58.0)	3 (60.0)	1 (14.3)	6 (33.3)	11 (52.4)		10 (34.5)	11 (52.4)	
> Mean age	21 (42.0)								
Sex	49 (98.0)	5 (100.0)	7 (100.0)	17 (100.0)	20 (95.2)	0.703	29 (100.0)	20 (95.2)	0.235
Male	1 (2.0)	0 (0.0)	0 (0.0)	0 (0.0)	1 (4.8)		0 (0.0)	1 (4.8)	
Female									
Mean tumor size (cm) (rang)	3.9 (1.5–7.5)	1 (20.0)	4 (57.1)	9 (52.9)	9 (42.9)	0.547	14 (48.3)	9 (42.9)	0.704
≤ Mean tumor size	23 (46.0)	4 (80.0)	3 (42.9)	8 (47.1)	12 (57.1)		15 (51.7)	12 (57.1)	
> Mean tumor size	27 (54.0)								
Histological grade	31 (62.0)	0 (0.0)	0 (0.0)	16 (94.1)	15 (71.4)	0.000	16 (55.2)	15 (71.4)	0.320
Well differentiated	17 (34.0)	4 (80.0)	7 (100.0)	0 (0.0)	6 (28.6)		11 (37.9)	6 (28.6)	
Moderate differentiated	2 (4.0)	1 (20.0)	0 (0.0)	1 (5.9)	0 (0.0)		2 (6.9)	0 (0.0)	
Poor differentiated									
Primary tumor (PT) stage	1 (2.0)	0 (0.0)	1 (14.3)	0 (0.0)	0 (0.0)	0.289	1 (3.4)	0 (0.0)	0.178
pT1	10 (20.0)	1 (20.0)	1 (14.3)	3 (17.6)	5 (23.8)		5 (17.2)	5 (23.8)	
pT2	22 (44.0)	3 (60.0)	4 (57.1)	9 (52.9)	6 (28.6)		16 (55.2)	6 (28.6)	
pT3	17 (34.0)	1 (20.0)	1 (14.3)	5 (29.4)	10 (47.6)		7 (24.1)	10 (47.6)	
pT4									
Lymphovascular invasion	2 (4.0)	0 (0.0)	0 (0.0)	1 (5.9)	1 (4.8)	0.876	1 (3.4)	1 (4.8)	0.815
Present	48 (96.0)	5 (100.0)	7 (100.0)	16 (94.1)	20 (95.2)		28 (96.6)	20 (95.2)	
Absent									

Characteristics of tumor	Total samples, N%	Intensity of staining *N* (%)				P value	H score (cut off = 120) N (%)		P value
		0 (Negative)	1 + (Weak)	2 + (Moderate)	3 + (Strong)		Low (< 120)	High (> 120)	
Perineural invasion	11 (22.0)	1 (20.0)	1 (14.3)	1 (5.9)	8 (38.1)	0.112	3 (10.3)	8 (38.1)	0.019
Present	39 (78.0)	4 (80.0)	6 (85.7)	16 (94.1)	13 (61.9)		26 (89.7)	13 (61.9)	
Absent									
Lymph node involvement	15 (30.0)	0 (0.0)	1 (14.3)	0 (0.0)	14 (66.7)	0.000	1 (3.4)	14 (66.7)	0.000
Yes	35 (70.0)	5 (100.0)	6 (85.7)	17 (100.0)	7 (33.3)		28 (96.6)	7 (33.3)	
No									

3.5. Evaluation of IDH1 R132H mutation in negative/weak positive staining intensities samples in laryngeal squamous cell carcinoma using PCR

To identify IDH1 R132H mutation, 12 LSCC samples with negative and weak positive staining intensities were assessed using gene sequencing with PCR technique. The IDH1 R132H exon4 sequencing results indicated that 11 of the 12 samples were negative for IDH1 R132H mutation and only one was positive (Fig. 7). Overall IDH1 R132H mutation were detected in 39 (78.0%) LSCC patients through using IHC and PCR methods. A flow chart of the process of samples selection is exhibited in Fig. 8.

3.6. Associations between status of IDH1 R132H mutation and clinicopathological features in laryngeal squamous cell carcinoma

All LSCC samples were divided into two groups, defined as positive IDH1 R132H or negative IDH1 R132H mutation. Pearson's $\chi 2$ test demonstrated a significant association between positive IDH1 mutation and histological grade ($p = 0.000$) as well as lymph node involvement ($p = 0.014$). We did not observe any association and correlation between the status of IDH1 R132H mutation and other clinicopathological characteristics. Furthermore, non-parametric Kruskal–Wallis and Mann–Whitney *U* tests were applied to evaluate differences between the tumor size among diverse IDH1 mutation groups. Our results did not display any differences between tumor size and various statuses of IDH1 R132H mutation (Table 4).

Table 4
The association between the status of IDH1 R132H mutation and clinicopathological characteristics of laryngeal squamous cell carcinoma patients

Characteristics of tumor	IDH1 R132H mutation, N (%)		*P value*
	Present	Absent	
Number of samples	39 (78.0)	11 (22.0)	
Mean age, years (SD)	61 (8.90)	60 (6.05)	0.673
Sex	38 (97.4)	11 (100.0)	0.592
Male	1 (2.6)	0 (0.0)	
Female			
Mean tumor size (cm) (SD)	3.90 (1.58)	3.97 (1.59)	0.878
Histological grade	31 (79.5)	0 (0.0)	0.000
Well differentiated	7 (17.9)	10 (90.9)	
Moderate differentiated	1 (2.6)	1 (9.1)	
Poor differentiated			
Primary tumor (PT) stage	0 (0.0)	1 (9.1)	0.175
pT1	8 (20.5)	2 (18.2)	
pT2	16 (41.0)	6 (54.5)	
pT3	15 (38.5)	2 (18.2)	
pT4			
Lymphovascular invasion	2 (5.1)	0 (0.0)	0.443
Present	37 (94.9)	11 (100.0)	
Absent			
Perineural invasion	10 (25.6)	1 (9.1)	0.242
Present	29 (74.4)	10 (90.9)	
Absent			
Lymph node involvement	15 (38.5)	0 (0.0)	0.014
Yes	24 (61.5)	11 (100.0)	
No			

4. Discussion

LSCC is one of the most common cancers of the respiratory system and head and neck region, accounting for 90–95 percent of all laryngeal cancers; its incidence has significantly increased in the last decade (2). Due to the lack of apparent symptoms in the early stage and the occurrence of lymph node metastases, the majority of patients present with advanced-stage cancer at diagnosis, which affects the prognosis of patients (39). In the early stages of the disease, LSCC can be treated with radical radiotherapy or surgery. However, advanced LSCC requires an integrated therapy plan

that includes radiation, surgery, chemotherapy, and follow-up approaches (40, 41). Given these facts and the limitations of currently available biomarkers, it appears crucial to explore more effective biomarkers that would help determine the appropriate treatment and monitoring of recurrence and metastasis precisely.

IDH1, a $NADP^+$ enzyme of the Krebs cycle, is localized in the cytoplasm and peroxisome, which converts isocitrate to α-KG (15). It participates in several cellular metabolic functions (lipid and glucose metabolism) and protects the cells from ROS and radiation (42). It has well-established roles in various types of cancers based on the DisGeNET database. Moreover, mutations of this gene in head and neck cancer tissues that led to alterations in IDH1 protein, as well as dysregulation in mRNA levels, were observed in tumor samples through online bioinformatics tools. Previous studies have shown that mutations in IDH1, especially R132H, the most common mutation (43), are detected in different types of malignancies, including cholangiocarcinoma, AML, and glioblastoma (22, 44, 45). Besides, its mutations are associated with several cancer-related processes, such as invasion, migration, and cell proliferation (46–48). It has an opposite dualistic role in survival rate; either overexpression of IDH1 worsens or improves survival (49, 50).

According to the STRING-PPI network, IDH1 was correlated with proteins that have important roles in cancer, such as ACO1, ACO2, GOT2, IDH3B, and OGDH. It has been reported that in highly glycolytic cancer cells, to survive under conditions of limited glucose and hypoxia, IDH1 and aconitase (ACO) are required to generate lipogenic citrate from glutamine-derived α-KG (35, 51). It has been found that germline mutations in IDH3B and Glutamic-oxaloacetic transaminase 2 (GOT2), a TCA cycle enzyme, along with IDH1 mutations, are involve in pheochromocytomas/paragangliomas predisposing and cancer metabolism through alterations in Krebs cycle metabolite ratios (36, 52). Moreover, it has been shown that IDH1 and oxoglutarate dehydrogenase (OGDH) are correlated with the development and progression of clear cell renal cell carcinoma (ccRCC) and serve as potential prognostic biomarkers (53).

Mutation in IDH1 leads to less binding to isocitrate and reduced formation of α-KG; Subsequently, it contributes to the formation of D2HG (13, 54, 55). The building up of D2HG is thought to function as an oncometabolite with a variety of potential tumorigenesities (56, 57). It has been established that D2HG has an α-KG antagonist role, which competitively inhibits α-KG-dependent dioxygenases due to the significant structural similarity that hydroxylates key proteins such as HIF-1α (54, 58, 59). Hence, in IDH1 mutant tumor cells, HIF-1α hydroxylation, a degradation enzyme, is inhibited and causes its upregulation in cancer cells (58, 60). High expression of HIF-1α is associated with tumor progression and a poor prognosis in cancers (61). Furthermore, 2HG augmentation prevents histone demethylation, resulting in histone hypermethylation and disruption of cell differentiation (62, 63). Also, the methylcytosine dioxygenase TET is inhibited by 2HG, leading to reduced 5-hydroxymethylcytosine and consequently impaired tumor differentiation (64, 65).

In addition, it has been found that IDH mutations are associated to the establishment and maintenance of cancer stem cells (CSCs). IDH mutations and IDH-related pathways may be important molecular targets for affecting CSC components in human malignancies and improving the prognosis of the disease (66).

The most prevalent IDH1 mutation is a heterozygous point mutation in which guanine is altered to adenine at position 395 (C.395G > A), resulting in the substitution of arginine at position 132 with histidine (R132H) at the IDH1 active site (22, 67). There is accumulating evidence indicating that IDH1 R132H (mIDH1) protein is expressed in several cancers with distinct regulatory signaling pathways. It has been reported that the IDH1 R132H mutation suppressed PTEN expression through activating the Notch1/HES1 and PI3K/AKT pathways, thereby promoting malignant behavior in T-cell acute lymphoblastic leukemia cells (68). In addition, the IDH1 R132H mutation downregulated ICAM-1/CD54 in glioma cells, representing an immunomodulation role of mutant IDH1 (69). It also contributes to the progression of non-small-cell lung cancer via promoting migration and proliferation (48). Thus, due to the existence of information gaps regarding the expression of IDH1 R132H in LSCC, in this study, for the first time, the expression level of IDH1 R132H was evaluated in

50 LSCC tissue samples as well as adjacent normal tissue. Further, the association between its expression levels and clinicopathological characteristics was assessed.

Our bioinformatics analysis revealed a modest difference in mRNA expression between LSCC and normal tissues, which is in accordance with our analysis of IHC, that showed that the cytoplasmic expression of IDH1 R132H is upregulated in adjacent normal tissues compared to LSCC samples. These findings are in agreement with several other studies regarding protein expression levels, including breast cancer, gastric cancer, and colorectal cancer (70, 71).

In the present study, the results of IHC revealed that low cytoplasmic expression of IDH1 R132H was found to be associated with advanced histological grade and high lymph node involvement. Furthermore, our results indicated that there is an adverse association between the cytoplasmic expression level of IDH1 R132H and increasing perineural invasion, while no association between the cytoplasmic expression of IDH1 R132H and other clinicopathological features was found.

There have been many contradictory reports concerning IDH1 expression and clinicopathological parameters in various tumor tissues. In accordance with our findings, previous studies revealed an inverse correlation between IDH1 expression and histological grade as well as lymph node involvement in colorectal cancer, gastric cancer, and ccRCC, suggesting high IDH1 expression can be an independent prognosis of favorable outcomes (71, 72). Besides, Liu, W.S. and colleagues discovered that low expression of IDH1 correlated with lymph node metastasis and high stage of breast cancer, leading to increased snail expression through activating HIF-1α and NFκB signaling. They identified that low expression of IDH1 could be an important marker for inhibiting cell migration and invasion of breast cancer cells (70).

It has been established that the IHC technique has 92.3% sensitivity, 97.9% specificity, and 96.7% accuracy, while PCR has 100% sensitivity, specificity, positive predictive values, negative predictive values, and accuracy to represent IDH1 mutation (73). Therefore, in order to confirm the negative IHC results, DNA sequencing of 12 LSCC tumor samples with negative and weak positive staining intensities was performed. As Gondim, D. D. and colleagues reported 3 false negative results from IHC in contrast to PCR results; we found 1 false negative (74). Our findings indicated that the IDH1 R132H mutation was observed in 78% of LSCC tumor samples, which consisted of 38 positive IHC results and 1 positive PCR. In this regard, previous studies have demonstrated that this mutation is present in a about 80% of grade II-III gliomas and secondary glioblastomas (43, 75, 76). As a result, IDH1 R132H immunostain is considered a first-line diagnostic test, and PCR could be used to examine non-immunoreactive samples (77). We suggest using both IHC and PCR to detect IDH1 mutations.

In general, our findings revealed the significance of IDH1 R132H in tumor cell invasion and cancer progression and introduced it as a potential for targeted cancer therapy. Indeed, IDH1 R132H, which is expressed in the cytoplasm at the protein level and is recognized by IHC and PCR methods, could be a specific predictive biomarker in LSCC. However, the limitations of this study are the small sample size and lack of survival data to investigate the prognostic role of IDH1 in LSCC. Extending the clinical follow-up time with a larger patient sample is recommended.

5. Conclusion

In summary the current study is the first to exhibit that decreased cytoplasmic expression of IDH1 has a clinical significance in LSCC cases and is associated with increased invasiveness and poor outcomes. Further, it is found that 78 percent of the LSCC tumor samples has IDH1 R132H mutations. To sum up, investigation of the expression pattern of IDH1 in the cytoplasm as a predictor indicator of cancer progression in LSCC patients' tumor biopsies is useful.

Declarations

Ethics approval and consent to participate

All procedures performed in this study were in line with the ethical standards of the institution at which this study was conducted. Informed consent was individually obtained from all participants. The Research Ethics Committee of Iran University of Medical Sciences issued IR.IUMS.FMD.REC.1399.276 for this study.

Informed consent was obtained from all individual participants, parents or legally authorized representatives of participants under legal age years old at the time of sample collection with routine consent forms.

Availability of data and materials

The analyzed data during the current study are available from the corresponding author on reasonable request.

Competing interests

The authors declare no conflict of interests.

Funding

This study was conducted as part of a resident thesis and was financially supported by a grant from the Department of Pathology, Iran University of Medical Sciences (IUMS) (Grant Number# 19921).

Authors' contributions

N.S, N.E, and F.T. designed and supervised the project, rechecked and approved all parts of the manuscript and data analysis; N.E., and F.T. wrote the manuscript. M.M. and A.M. collected the paraffin-embedded tissues, collected the patient data, and performed an IHC experiment. A.Z.M. analyzed and interpreted the SPSS data and helped to prepare the tables. N.S. marked the most representative areas in different parts of the tumor for the construction of TMAs blocks and scored TMAs slides after IHC staining, and helped to prepare the figures. E.J. performed PCR and analyzed the results of PCR. All authors read and approved the final manuscript.

References

1. Sung H, Ferlay J, Siegel RL, Laversanne M, Soerjomataram I, Jemal A, et al. Global Cancer Statistics 2020: GLOBOCAN Estimates of Incidence and Mortality Worldwide for 36 Cancers in 185 Countries. CA Cancer J Clin. 2021;71(3):209–49.
2. Siegel RL, Miller KD, Fuchs HE, Jemal A. Cancer statistics, 2022. CA Cancer J Clin. 2022;72(1):7–33.
3. Johnson DE, Burtness B, Leemans CR, Lui VWY, Bauman JE, Grandis JR. Head and neck squamous cell carcinoma. Nat Rev Dis Primers. 2020;6(1):92.
4. Forastiere AA, Ismaila N, Lewin JS, Nathan CA, Adelstein DJ, Eisbruch A, et al. Use of Larynx-Preservation Strategies in the Treatment of Laryngeal Cancer: American Society of Clinical Oncology Clinical Practice Guideline Update. J Clin Oncol. 2018;36(11):1143–69.
5. Carlisle JW, Steuer CE, Owonikoko TK, Saba NF. An update on the immune landscape in lung and head and neck cancers. CA Cancer J Clin. 2020;70(6):505–17.
6. Megwalu UC, Sikora AG. Survival outcomes in advanced laryngeal cancer. JAMA Otolaryngol Head Neck Surg. 2014;140(9):855–60.
7. Al-Khallaf H. Isocitrate dehydrogenases in physiology and cancer: biochemical and molecular insight. Cell Biosci. 2017;7:37-.

8. Stoddard BL, Dean A, Koshland DE, Jr. Structure of isocitrate dehydrogenase with isocitrate, nicotinamide adenine dinucleotide phosphate, and calcium at 2.5-A resolution: a pseudo-Michaelis ternary complex. Biochemistry. 1993;32(36):9310–6.
9. Tommasini-Ghelfi S, Murnan K, Kouri FM, Mahajan AS, May JL, Stegh AH. Cancer-associated mutation and beyond: The emerging biology of isocitrate dehydrogenases in human disease. Sci Adv. 2019;5(5):eaaw4543-eaaw.
10. Reitman ZJ, Yan H. Isocitrate dehydrogenase 1 and 2 mutations in cancer: alterations at a crossroads of cellular metabolism. J Natl Cancer Inst. 2010;102(13):932–41.
11. Ronnebaum SM, Ilkayeva O, Burgess SC, Joseph JW, Lu D, Stevens RD, et al. A pyruvate cycling pathway involving cytosolic NADP-dependent isocitrate dehydrogenase regulates glucose-stimulated insulin secretion. J Biol Chem. 2006;281(41):30593–602.
12. Molenaar RJ, Radivoyevitch T, Maciejewski JP, van Noorden CJ, Bleeker FE. The driver and passenger effects of isocitrate dehydrogenase 1 and 2 mutations in oncogenesis and survival prolongation. Biochim Biophys Acta. 2014;1846(2):326–41.
13. Dang L, White DW, Gross S, Bennett BD, Bittinger MA, Driggers EM, et al. Cancer-associated IDH1 mutations produce 2-hydroxyglutarate. Nature. 2009;462(7274):739–44.
14. Robertson FL, Marqués-Torrejón MA, Morrison GM, Pollard SM. Experimental models and tools to tackle glioblastoma. Dis Model Mech. 2019;12(9).
15. Xu X, Zhao J, Xu Z, Peng B, Huang Q, Arnold E, et al. Structures of human cytosolic NADP-dependent isocitrate dehydrogenase reveal a novel self-regulatory mechanism of activity. J Biol Chem. 2004;279(32):33946–57.
16. Cairns RA, Mak TW. Oncogenic isocitrate dehydrogenase mutations: mechanisms, models, and clinical opportunities. Cancer Discov. 2013;3(7):730–41.
17. Paschka P, Schlenk RF, Gaidzik VI, Habdank M, Krönke J, Bullinger L, et al. IDH1 and IDH2 mutations are frequent genetic alterations in acute myeloid leukemia and confer adverse prognosis in cytogenetically normal acute myeloid leukemia with NPM1 mutation without FLT3 internal tandem duplication. J Clin Oncol. 2010;28(22):3636–43.
18. Yan H, Parsons DW, Jin G, McLendon R, Rasheed BA, Yuan W, et al. IDH1 and IDH2 mutations in gliomas. New England journal of medicine. 2009;360(8):765–73.
19. Chotirat S, Thongnoppakhun W, Promsuwicha O, Boonthimat C, Auewarakul CU. Molecular alterations of isocitrate dehydrogenase 1 and 2 (IDH1 and IDH2) metabolic genes and additional genetic mutations in newly diagnosed acute myeloid leukemia patients. J Hematol Oncol. 2012;5:5.
20. Yang H, Ye D, Guan KL, Xiong Y. IDH1 and IDH2 mutations in tumorigenesis: mechanistic insights and clinical perspectives. Clin Cancer Res. 2012;18(20):5562–71.
21. Sjöblom T, Jones S, Wood LD, Parsons DW, Lin J, Barber TD, et al. The consensus coding sequences of human breast and colorectal cancers. Science. 2006;314(5797):268–74.
22. Parsons DW, Jones S, Zhang X, Lin JC, Leary RJ, Angenendt P, et al. An integrated genomic analysis of human glioblastoma multiforme. Science. 2008;321(5897):1807–12.
23. Kloosterhof NK, Bralten LB, Dubbink HJ, French PJ, van den Bent MJ. Isocitrate dehydrogenase-1 mutations: a fundamentally new understanding of diffuse glioma? The lancet oncology. 2011;12(1):83–91.
24. Mardis ER, Ding L, Dooling DJ, Larson DE, McLellan MD, Chen K, et al. Recurring mutations found by sequencing an acute myeloid leukemia genome. New England Journal of Medicine. 2009;361(11):1058–66.
25. Shibata T, Kokubu A, Miyamoto M, Sasajima Y, Yamazaki N. Mutant IDH1 confers an in vivo growth in a melanoma cell line with BRAF mutation. The American journal of pathology. 2011;178(3):1395–402.
26. Amary MF, Bacsi K, Maggiani F, Damato S, Halai D, Berisha F, et al. IDH1 and IDH2 mutations are frequent events in central chondrosarcoma and central and periosteal chondromas but not in other mesenchymal tumours. The Journal

of pathology. 2011;224(3):334–43.
27. Ghiam A, Cairns R, Thoms J, Dal Pra A, Ahmed O, Meng A, et al. IDH mutation status in prostate cancer. Oncogene. 2012;31(33):3826-.
28. Borger DR, Tanabe KK, Fan KC, Lopez HU, Fantin VR, Straley KS, et al. Frequent mutation of isocitrate dehydrogenase (IDH) 1 and IDH2 in cholangiocarcinoma identified through broad-based tumor genotyping. The oncologist. 2012;17(1):72–9.
29. Tallegas M, Miquelestorena-Standley É, Labit-Bouvier C, Badoual C, Francois A, Gomez-Brouchet A, et al. IDH mutation status in a series of 88 head and neck chondrosarcomas: different profile between tumors of the skull base and tumors involving the facial skeleton and the laryngotracheal tract. Hum Pathol. 2019;84:183–91.
30. Cerami E, Gao J, Dogrusoz U, Gross BE, Sumer SO, Aksoy BA, et al. The cBio cancer genomics portal: an open platform for exploring multidimensional cancer genomics data. Cancer Discov. 2012;2(5):401–4.
31. Goldman M, Craft B, Hastie M, Repečka K, Kamath A, McDade F, et al. The UCSC Xena platform for public and private cancer genomics data visualization and interpretation. bioRxiv. 2019:326470.
32. Piñero J, Ramírez-Anguita JM, Saüch-Pitarch J, Ronzano F, Centeno E, Sanz F, et al. The DisGeNET knowledge platform for disease genomics: 2019 update. Nucleic acids research. 2020;48(D1):D845-D55.
33. Doncheva NT, Morris JH, Gorodkin J, Jensen LJ. Cytoscape StringApp: Network Analysis and Visualization of Proteomics Data. Journal of proteome research. 2019;18(2):623–32.
34. Shannon P, Markiel A, Ozier O, Baliga NS, Wang JT, Ramage D, et al. Cytoscape: a software environment for integrated models of biomolecular interaction networks. Genome research. 2003;13(11):2498–504.
35. Smolková K, Ježek P. The Role of Mitochondrial NADPH-Dependent Isocitrate Dehydrogenase in Cancer Cells. Int J Cell Biol. 2012;2012:273947.
36. Remacha L, Comino-Méndez I, Richter S, Contreras L, Currás-Freixes M, Pita G, et al. Targeted Exome Sequencing of Krebs Cycle Genes Reveals Candidate Cancer-Predisposing Mutations in Pheochromocytomas and Paragangliomas. Clin Cancer Res. 2017;23(20):6315–24.
37. Dang L, Yen K, Attar EC. IDH mutations in cancer and progress toward development of targeted therapeutics. Annals of Oncology. 2016;27(4):599–608.
38. Shait Mohammed MR, Alzahrani F, Hosawi S, Choudhry H, Khan MI. Profiling the Effect of Targeting Wild Isocitrate Dehydrogenase 1 (IDH1) on the Cellular Metabolome of Leukemic Cells. Int J Mol Sci. 2022;23(12).
39. Cooper JS, Pajak TF, Forastiere AA, Jacobs J, Campbell BH, Saxman SB, et al. Postoperative concurrent radiotherapy and chemotherapy for high-risk squamous-cell carcinoma of the head and neck. N Engl J Med. 2004;350(19):1937–44.
40. Orlandi E, Iacovelli NA, Tombolini V, Rancati T, Polimeni A, De Cecco L, et al. Potential role of microbiome in oncogenesis, outcome prediction and therapeutic targeting for head and neck cancer. Oral Oncol. 2019;99:104453.
41. Niu H, Zhu Y, Wang J, Wang T, Wang X, Yan L. Effects of USP7 on radiation sensitivity through p53 pathway in laryngeal squamous cell carcinoma. Transl Oncol. 2022;22:101466.
42. Lee SM, Koh HJ, Park DC, Song BJ, Huh TL, Park JW. Cytosolic NADP(+)-dependent isocitrate dehydrogenase status modulates oxidative damage to cells. Free Radic Biol Med. 2002;32(11):1185–96.
43. Bleeker FE, Lamba S, Leenstra S, Troost D, Hulsebos T, Vandertop WP, et al. IDH1 mutations at residue p.R132 (IDH1(R132)) occur frequently in high-grade gliomas but not in other solid tumors. Hum Mutat. 2009;30(1):7–11.
44. Zhou B, Yang F, Qin L, Kuai J, Yang L, Zhang L, et al. Computational study on novel natural compound inhibitor targeting IDH1_R132H. Aging (Albany NY). 2022;14(undefined).
45. Marcucci G, Maharry K, Wu YZ, Radmacher MD, Mrózek K, Margeson D, et al. IDH1 and IDH2 gene mutations identify novel molecular subsets within de novo cytogenetically normal acute myeloid leukemia: a Cancer and Leukemia

Group B study. J Clin Oncol. 2010;28(14):2348–55.

46. Xu H, Sun Y, You B, Huang CP, Ye D, Chang C. Androgen receptor reverses the oncometabolite R-2-hydroxyglutarate-induced prostate cancer cell invasion via suppressing the circRNA-51217/miRNA-646/TGFβ1/p-Smad2/3 signaling. Cancer Lett. 2020;472:151–64.
47. Shen X, Wu S, Zhang J, Li M, Xu F, Wang A, et al. Wild–type IDH1 affects cell migration by modulating the PI3K/AKT/mTOR pathway in primary glioblastoma cells. Mol Med Rep. 2020;22(3):1949–57.
48. Yan B, Hu Y, Ma T, Wang Y. IDH1 mutation promotes lung cancer cell proliferation through methylation of Fibulin-5. Open Biol. 2018;8(10).
49. Lugowska I, Teterycz P, Mikula M, Kulecka M, Kluska A, Balabas A, et al. IDH1/2 Mutations Predict Shorter Survival in Chondrosarcoma. J Cancer. 2018;9(6):998–1005.
50. Alghamri MS, Thalla R, Avvari RP, Dabaja A, Taher A, Zhao L, et al. Tumor mutational burden predicts survival in patients with low-grade gliomas expressing mutated IDH1. Neurooncol Adv. 2020;2(1):vdaa042.
51. Metallo CM, Gameiro PA, Bell EL, Mattaini KR, Yang J, Hiller K, et al. Reductive glutamine metabolism by IDH1 mediates lipogenesis under hypoxia. Nature. 2011;481(7381):380–4.
52. Lane AN, Higashi RM, Fan TW. Metabolic reprogramming in tumors: Contributions of the tumor microenvironment. Genes Dis. 2020;7(2):185–98.
53. Zhang Y, Chen M, Liu M, Xu Y, Wu G. Glycolysis-Related Genes Serve as Potential Prognostic Biomarkers in Clear Cell Renal Cell Carcinoma. Oxid Med Cell Longev. 2021;2021:6699808.
54. Zhao S, Lin Y, Xu W, Jiang W, Zha Z, Wang P, et al. Glioma-derived mutations in IDH1 dominantly inhibit IDH1 catalytic activity and induce HIF-1alpha. Science. 2009;324(5924):261–5.
55. Pietrak B, Zhao H, Qi H, Quinn C, Gao E, Boyer JG, et al. A tale of two subunits: how the neomorphic R132H IDH1 mutation enhances production of αHG. Biochemistry. 2011;50(21):4804–12.
56. DiNardo CD, Propert KJ, Loren AW, Paietta E, Sun Z, Levine RL, et al. Serum 2-hydroxyglutarate levels predict isocitrate dehydrogenase mutations and clinical outcome in acute myeloid leukemia. Blood. 2013;121(24):4917–24.
57. Ward PS, Cross JR, Lu C, Weigert O, Abel-Wahab O, Levine RL, et al. Identification of additional IDH mutations associated with oncometabolite R(-)-2-hydroxyglutarate production. Oncogene. 2012;31(19):2491–8.
58. Xu W, Yang H, Liu Y, Yang Y, Wang P, Kim SH, et al. Oncometabolite 2-hydroxyglutarate is a competitive inhibitor of α-ketoglutarate-dependent dioxygenases. Cancer Cell. 2011;19(1):17–30.
59. Jiang B, Zhao W, Shi M, Zhang J, Chen A, Ma H, et al. IDH1 Arg-132 mutant promotes tumor formation through down-regulating p53. J Biol Chem. 2018;293(25):9747–58.
60. Sasaki M, Knobbe CB, Itsumi M, Elia AJ, Harris IS, Chio, II, et al. D-2-hydroxyglutarate produced by mutant IDH1 perturbs collagen maturation and basement membrane function. Genes Dev. 2012;26(18):2038–49.
61. Metellus P, Colin C, Taieb D, Guedj E, Nanni-Metellus I, de Paula AM, et al. IDH mutation status impact on in vivo hypoxia biomarkers expression: new insights from a clinical, nuclear imaging and immunohistochemical study in 33 glioma patients. J Neurooncol. 2011;105(3):591–600.
62. Lu C, Ward PS, Kapoor GS, Rohle D, Turcan S, Abdel-Wahab O, et al. IDH mutation impairs histone demethylation and results in a block to cell differentiation. Nature. 2012;483(7390):474–8.
63. Krell D, Mulholland P, Frampton AE, Krell J, Stebbing J, Bardella C. IDH mutations in tumorigenesis and their potential role as novel therapeutic targets. Future Oncol. 2013;9(12):1923–35.
64. Guo JU, Su Y, Zhong C, Ming GL, Song H. Emerging roles of TET proteins and 5-hydroxymethylcytosines in active DNA demethylation and beyond. Cell Cycle. 2011;10(16):2662–8.
65. Figueroa ME, Abdel-Wahab O, Lu C, Ward PS, Patel J, Shih A, et al. Leukemic IDH1 and IDH2 mutations result in a hypermethylation phenotype, disrupt TET2 function, and impair hematopoietic differentiation. Cancer Cell.

2010;18(6):553–67.
66. Zhang Y, Liu Y, Lang F, Yang C. IDH mutation and cancer stem cell. Essays Biochem. 2022.
67. Olar A, Raghunathan A, Albarracin CT, Aldape KD, Cahill DP, 3rd, Powell SZ, et al. Absence of IDH1-R132H mutation predicts rapid progression of nonenhancing diffuse glioma in older adults. Ann Diagn Pathol. 2012;16(3):161–70.
68. Liu Y, Fang B, Feng X, Jiang Y, Zeng Y, Jiang J. Mechanism of IDH1-R132H mutation in T cell acute lymphoblastic leukemia mouse model via the Notch1 pathway. Tissue Cell. 2022;74:101674.
69. Ma D, Zhan D, Fu Y, Wei S, Lal B, Wang J, et al. Mutant IDH1 promotes phagocytic function of microglia/macrophages in gliomas by downregulating ICAM1. Cancer Lett. 2021;517:35–45.
70. Liu WS, Chan SH, Chang HT, Li GC, Tu YT, Tseng HH, et al. Isocitrate dehydrogenase 1-snail axis dysfunction significantly correlates with breast cancer prognosis and regulates cell invasion ability. Breast Cancer Res. 2018;20(1):25.
71. Li J, Huang J, Huang F, Jin Q, Zhu H, Wang X, et al. Decreased expression of IDH1-R132H correlates with poor survival in gastrointestinal cancer. Oncotarget. 2016;7(45):73638–50.
72. Laba P, Wang J, Zhang J. Low level of isocitrate dehydrogenase 1 predicts unfavorable postoperative outcomes in patients with clear cell renal cell carcinoma. BMC Cancer. 2018;18(1):852.
73. Malueka RG, Theresia E, Fitria F, Argo IW, Donurizki AD, Shaleh S, et al. Comparison of Polymerase Chain Reaction-Restriction Fragment Length Polymorphism, Immunohistochemistry, and DNA Sequencing for the Detection of IDH1 Mutations in Gliomas. Asian Pac J Cancer Prev. 2020;21(11):3229–34.
74. Gondim DD, Gener MA, Curless KL, Cohen-Gadol AA, Hattab EM, Cheng L. Determining IDH-Mutational Status in Gliomas Using IDH1-R132H Antibody and Polymerase Chain Reaction. Appl Immunohistochem Mol Morphol. 2019;27(10):722–5.
75. Balss J, Meyer J, Mueller W, Korshunov A, Hartmann C, von Deimling A. Analysis of the IDH1 codon 132 mutation in brain tumors. Acta Neuropathol. 2008;116(6):597–602.
76. Kang MR, Kim MS, Oh JE, Kim YR, Song SY, Seo SI, et al. Mutational analysis of IDH1 codon 132 in glioblastomas and other common cancers. Int J Cancer. 2009;125(2):353–5.
77. Sporikova Z, Slavkovsky R, Tuckova L, Kalita O, Megova Houdova M, Ehrmann J, et al. IDH1/2 Mutations in Patients With Diffuse Gliomas: A Single Centre Retrospective Massively Parallel Sequencing Analysis. Appl Immunohistochem Mol Morphol. 2022;30(3):178–83.

Figures

A

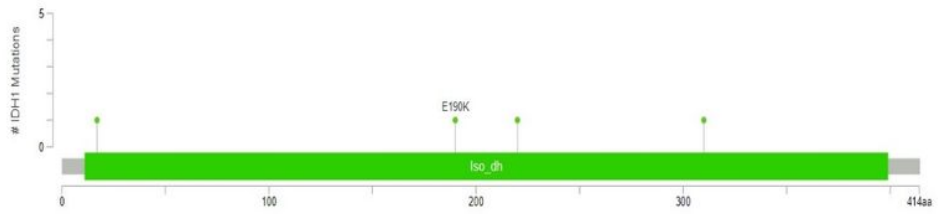

B

10 Mutations: includes 6 duplicate mutations in patients with multiple samples (page 1 of 1)

Study of Origin	Protein Change	Mutation Type	Copy #	Allele Freq (T)	Exon (10 in total)
Head and Neck Squamous Cell Carcinoma (TCGA, PanCancer Atlas)	*E17K*	Missense	ShallowDel	0.44	3
Head and Neck Squamous Cell Carcinoma (TCGA, Nature 2015)	*E17K*	Missense	ShallowDel	0.47	3
Head and Neck Squamous Cell Carcinoma (TCGA, Firehose Legacy)	*E17K*	Missense	ShallowDel	0.47	3
Head and Neck Squamous Cell Carcinoma (TCGA, PanCancer Atlas)	*E190K*	Missense	ShallowDel	0.40	6
Head and Neck Squamous Cell Carcinoma (TCGA, Nature 2015)	*E190K*	Missense	Diploid	0.41	6
Head and Neck Squamous Cell Carcinoma (TCGA, Firehose Legacy)	*E190K*	Missense	ShallowDel	0.41	6
Head and Neck Squamous Cell Carcinoma (TCGA, PanCancer Atlas)	*D220N*	Missense	Diploid	0.11	6
Head and Neck Squamous Cell Carcinoma (TCGA, Firehose Legacy)	*D220N*	Missense	Diploid	0.12	6
Head and Neck Squamous Cell Carcinoma (TCGA, PanCancer Atlas)	*G310V*	Missense	Gain	0.25	8
Head and Neck Squamous Cell Carcinoma (TCGA, Firehose Legacy)	*G310V*	Missense	Gain	0.25	8

Figure 1

IDH1 mutations in 5 head and neck cancer studies (cBioPortal). A) This graphical view shows the protein domains and the positions of mutations. B) The frequency and information for missense mutation type in the IDH1 gene that leads to 5 changes in its protein.

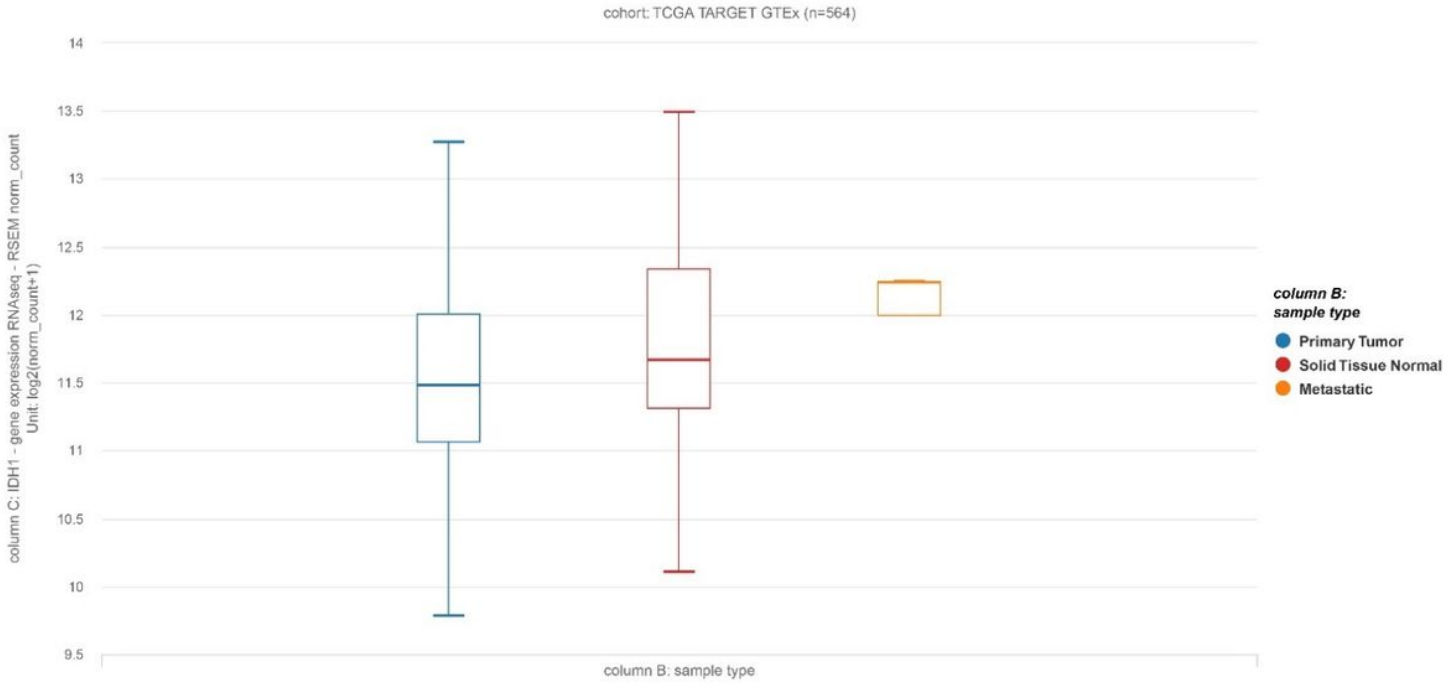

Figure 2

Box plot results of IDH1 expression for head and neck cancer compared to normal tissues through the UCSC Xena platform. The results showed an increased expression of IDH1 expression in head and neck tumor tissues compared to normal tissue although was not a statistically significant association (P > 0.05).

Figure 3

Protein-protein interaction (PPI) network for IDH1 protein. PPI network for IDH1 protein was created by StringApp plug-in using Cytoscape software with a confidence score ≥ 0.4.

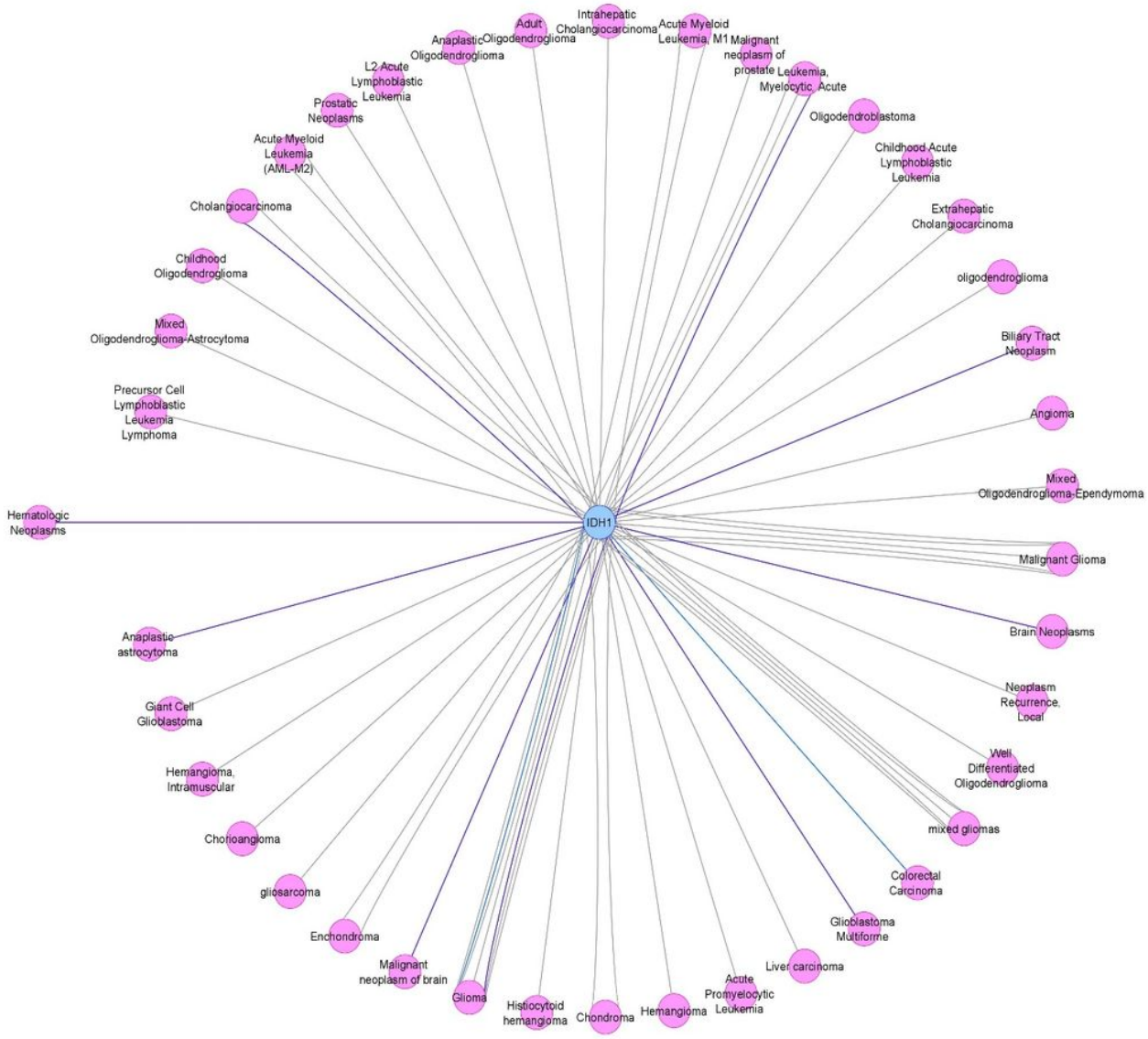

Figure 4

Obtained data about IDH1 in the DisGeNET library. Investigation of the IDH1 gene based on the DisGeNET database by Cytoscape shows that this gene is involved in various cancer.

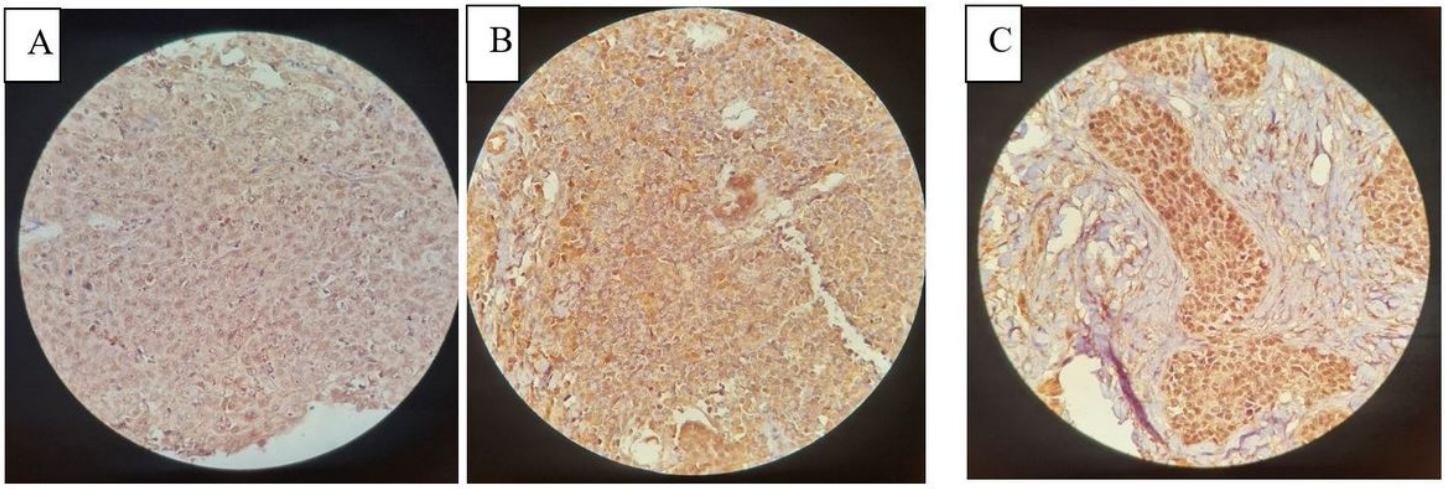

Figure 5

Immunohistochemistry staining for IDH1 R132H expression in laryngeal squamous cell carcinoma samples. LSCC samples expressed IDH1 R132H at various levels. There was **(A)** weak, **(B)** moderate and **(C)** strong immunoreactivity in the cytoplasmic expression of IDH1 R132H in LSCC tissue samples.

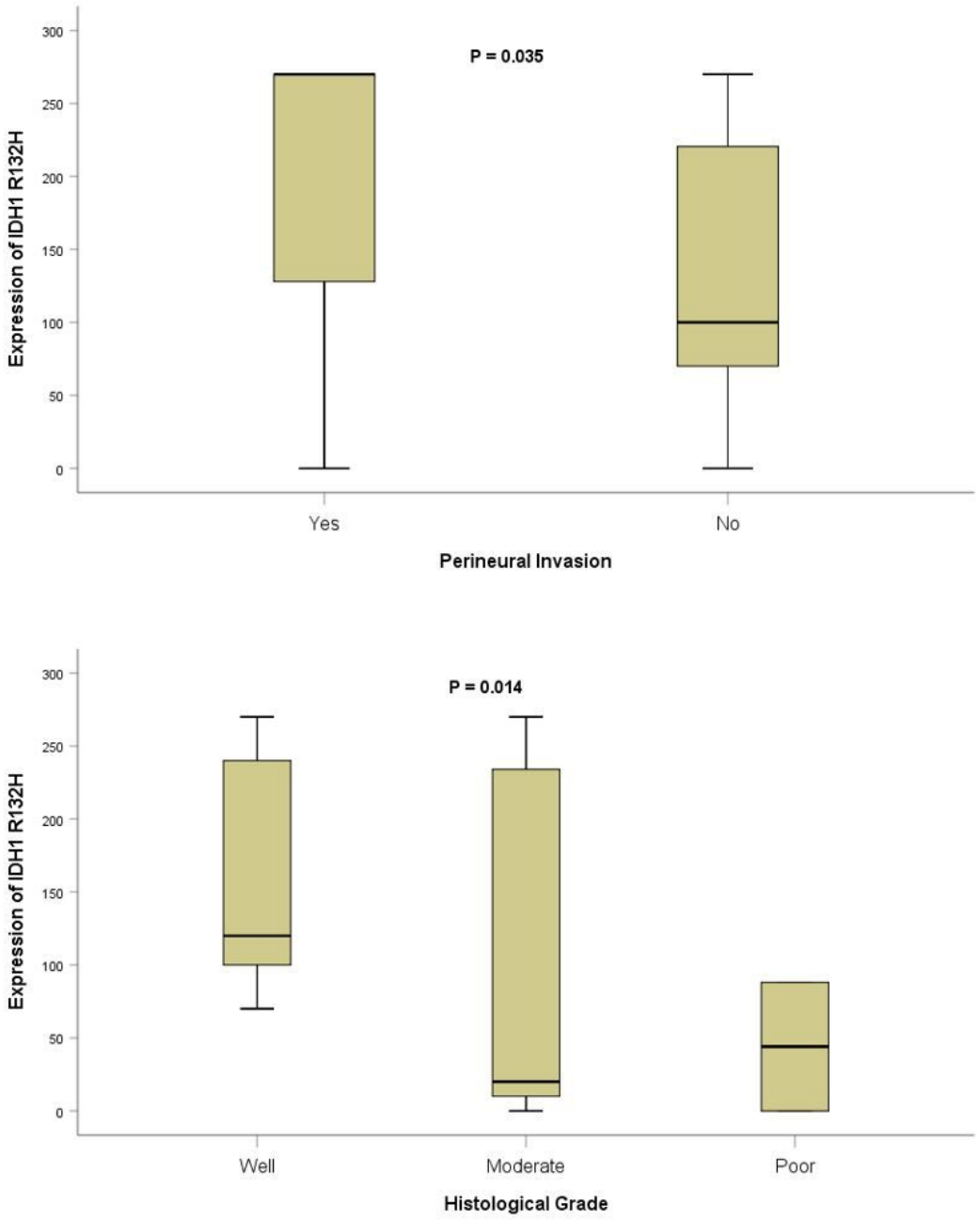

Figure 6

Box plot analysis of expression levels of IDH1 R132H in perineural invasion and histological grade in laryngeal squamous cell carcinoma (LSCC) using Kruskal–Wallis and Mann–Whitney U tests. Based on the standard definitions, each box plot shows the mean (bold line) and interquartile lines (box). The results showed that there was a statistically significant association between the mean of IDH1 R132H expression and **A**. perineural invasion patients (*p = 0.035*) **B.** as well as histological grade (*p = 0.014*).

Figure 7

Genomic Sequencing Results Showing **(A)** positive and **(B)** negative IDH1 R132H mutation

Figure 8

flow chart of the process of samples selection for IHC and PCR